Geoscientific
Model Development

Supplement of

Improved tropospheric and stratospheric sulfur cycle in the aerosol–chemistry–climate model SOCOL-AERv2

Aryeh Feinberg et al.

Correspondence to: Aryeh Feinberg (aryeh.feinberg@env.ethz.ch)

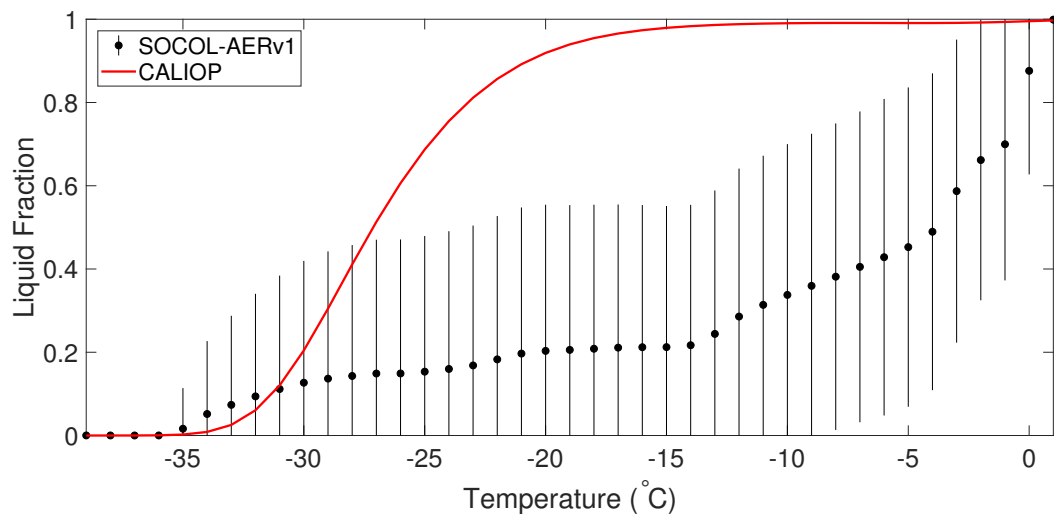**Figure S1:** The liquid fraction of clouds in the mixed-phase cloud regime ($-38\,°\text{C} < T < 0\,°\text{C}$) simulated by SOCOL-AERv1 based on ECHAM5 during a one-year simulation (solid circles). 12-hourly model output in all grid boxes with clouds is averaged in 1 degree temperature bins, with standard deviation bars included. The red curve shows the fitted sigmoid function (Hu et al., 2010) for the supercooled liquid fraction, SLF_{Hu}, derived from CALIOP Lidar measurements on board of the CALIPSO satellite. In its aqueous chemistry scheme, SOCOL-AERv2 adopts the satellite SLF to calculate the liquid water content from the model's total water content, $\text{LWC} = \text{SLF}_{\text{Hu}} \times \text{TWC}$.
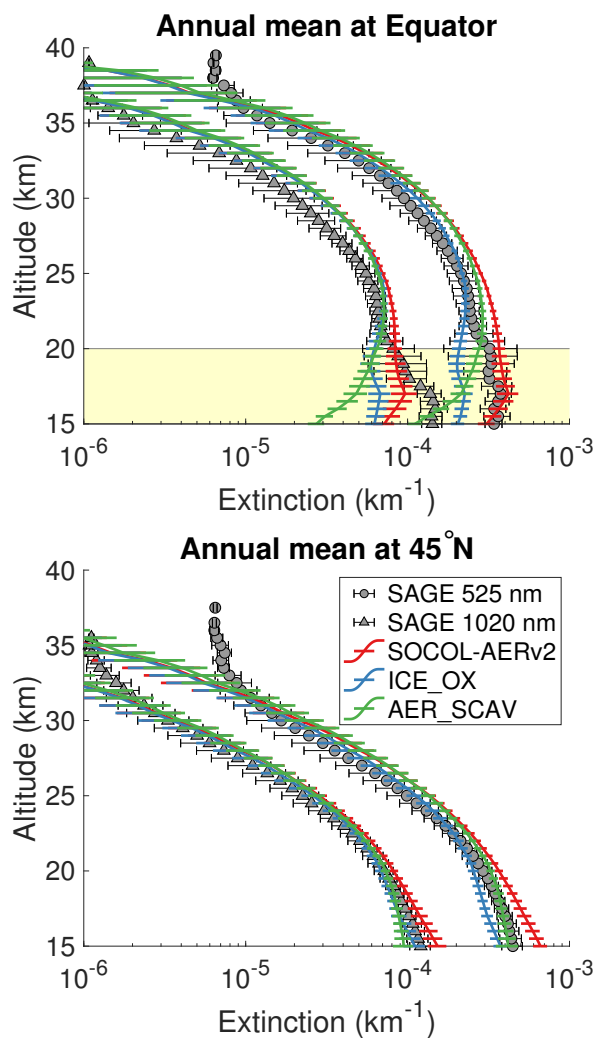
Figure S2: Comparison between annual mean model extinctions at 525 and 1020 nm and SAGE II measurements from the GloSSAC project (Thomason et al., 2018) at the Equator (*top*) and 45° N (*bottom*). Observations are averaged between 2000–2004, representing the volcanically quiescent part of the record. Model results are averaged over 5 years of the year 2000 time-slice for SOCOL-AERv2, ICE_OX, and AER_SCAV. Horizontal bars represent the modelled or observed standard deviation. The highlighted region in the upper plot corresponds to the altitudes where non-sulfate aerosols may play a role.
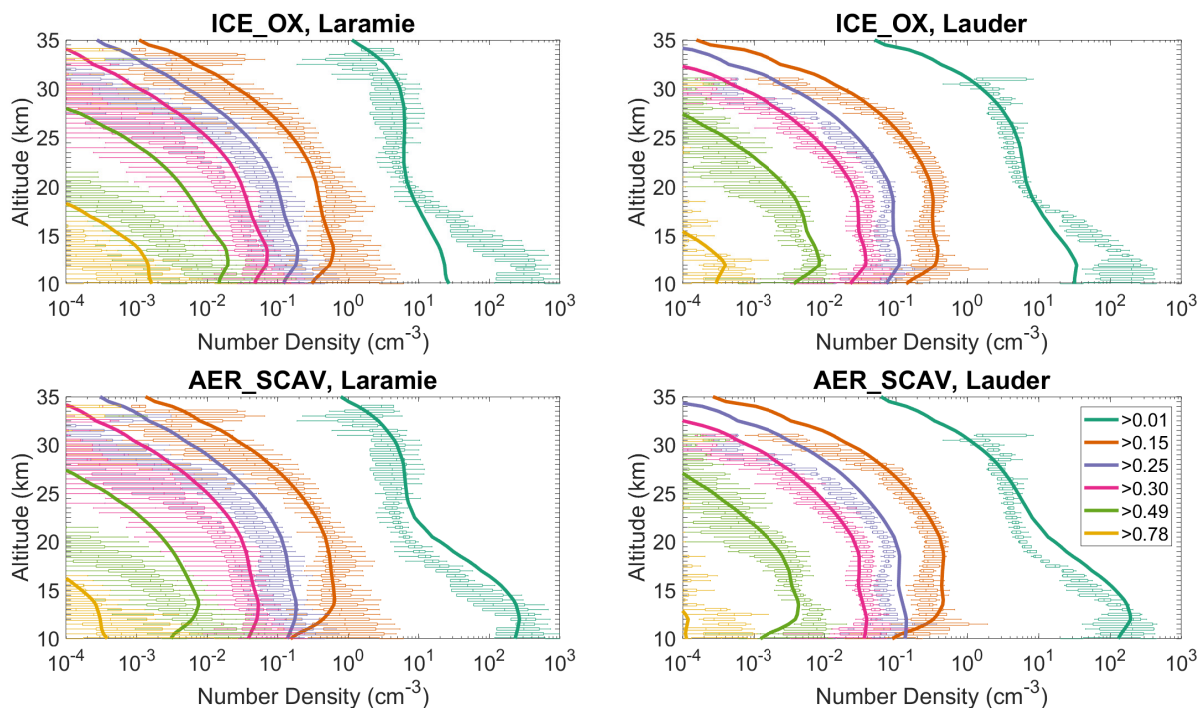
Figure S3: Number densities of particle size bins measured by OPC (Deshler et al., 2003; Deshler, 2008) and modelled by ICE_OX and AER_SCAV over Laramie, Wyoming, USA (41° N, 105° W) and Lauder, New Zealand (45° S, 170° W). Measured number densities are shown as box plots (minimum excluding outliers below the 0.4 percentile, 25th percentile, median, 75th percentile, maximum excluding outliers above the 99.6 percentile) and modelled number densities as solid lines. For the Laramie plots (*left*), OPC measurements are used from the period 1999–2008 and zonal mean model results are averaged over the 5 years of the time-slice. For the Lauder plots (*right*), OPC measurements are used from January to April 1998–2001 and zonal mean model results are averaged from January to April over 5 years of the time-slice. Model results are weighted with the counting efficiencies for OPC channels from Deshler et al. (2019) for direct comparability with the measurements.
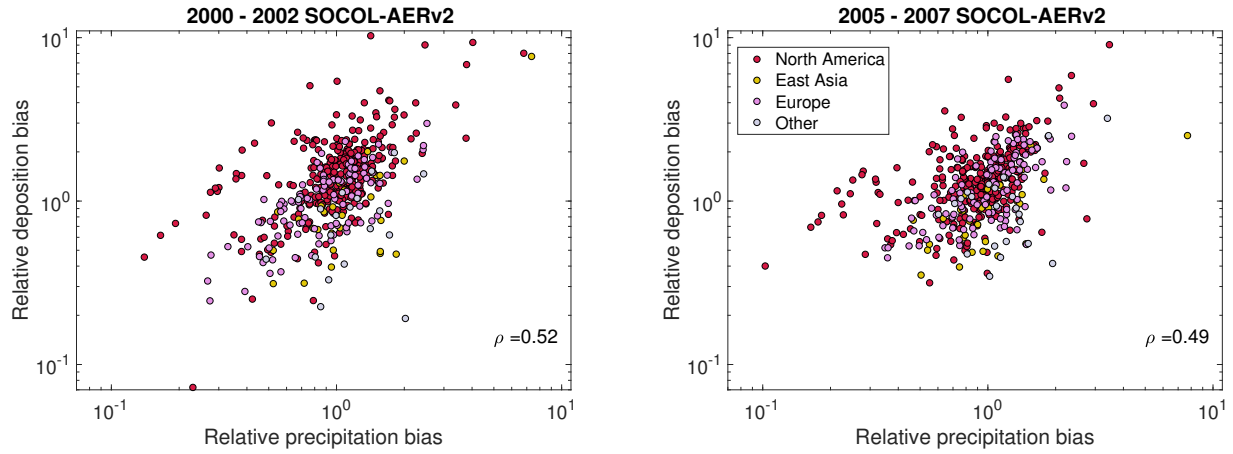
Figure S4: Comparison of modelled biases, relative to measurement sites from the WMO database (Vet et al., 2014), in precipitation and deposition. SOCOL-AERv2 is compared with measurements in two different time periods, 2000–2002 and 2005–2007. The Spearman correlation coefficient is listed on each plot.
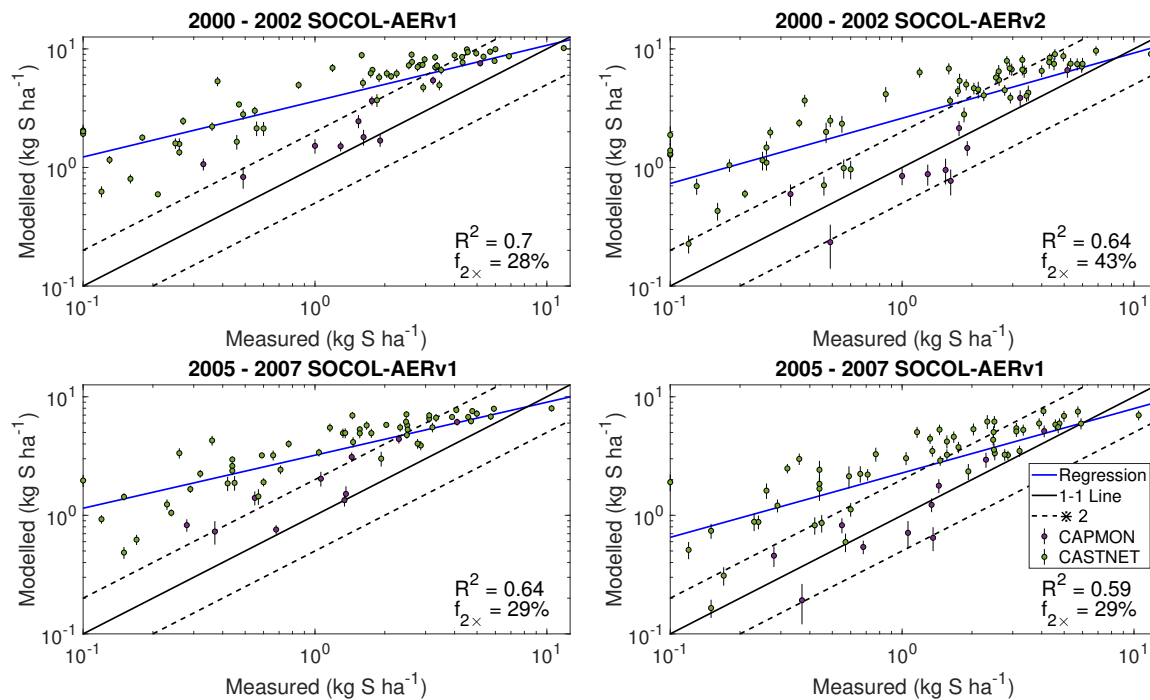
Figure S5: Evaluation of modelled SO_2 dry deposition against North American measurement sites from the WMO database (Vet et al., 2014). SOCOL-AERv1 and SOCOL-AERv2 are compared with measurements in two different time periods, 2000–2002 and 2005–2007. The ensemble standard deviation for the model results is shown as vertical bars. A power regression between the simulation results and measurements is shown in blue, and can be compared to the one-to-one line shown in black. Two model evaluation metrics are listed on the plots: the goodness of fit of the power regression between model and measurements (R^2) and the fraction of sites for which the model is within a factor of 2 of measurements ($f_{2\times}$). Points are colored according to the measurement network of the sites.
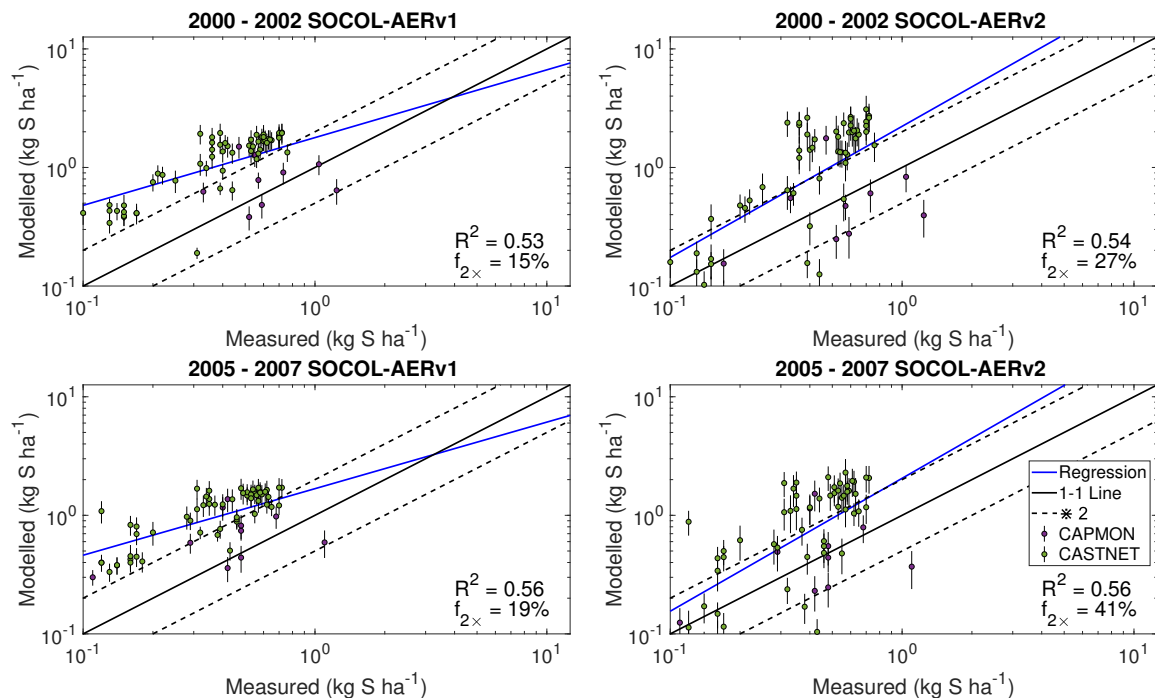
Figure S6: Evaluation of modelled sulfate aerosol dry deposition against North American measurement sites from the WMO database (Vet et al., 2014). SOCOL-AERv1 and SOCOL-AERv2 are compared with measurements in two different time periods, 2000–2002 and 2005–2007. The ensemble standard deviation for the model results is shown as vertical bars. A power regression between the simulation results and measurements is shown in blue, and can be compared to the one-to-one line shown in black. Two model evaluation metrics are listed on the plots: the goodness of fit of the power regression between model and measurements (R^2) and the the fraction of sites for which the model is within a factor of 2 of measurements ($f_{2\times}$). Points are colored according to the measurement network of the sites.

Table S1: The time periods covered by model intercomparison projects of sulfur deposition and this study.

Project Name	Simulation Period	Observation Period	Reference
Photocomp	2000	2000	Dentener et al. (2006)
ACCMIP	2000	2000–2002	Lamarque et al. (2013)
HTAP I	2001	2000–2002	Vet et al. (2014)
HTAP II	2010	2009–2011	Tan et al. (2018)
SOCOL-AERv2	2000–2002	2000–2002	This study
	2000–2002	2005–2007	

S1 References

Dentener, F., Drevet, J., Lamarque, J.-F., Bey, I., Eickhout, B., Fiore, A. M., Hauglustaine, D., Horowitz, L. W., Krol, M., and Kulshrestha, U.: Nitrogen and sulfur deposition on regional and global scales: A multimodel evaluation, Global biogeochemical cycles, 20, 2006.

Deshler, T.: A review of global stratospheric aerosol: Measurements, importance, life cycle, and local stratospheric aerosol, Atmospheric Research, 90, 223–232, 2008.

Deshler, T., Hervig, M., Hofmann, D., Rosen, J., and Liley, J.: Thirty years of in situ stratospheric aerosol size distribution measurements from Laramie, Wyoming (41 N), using balloonborne instruments, Journal of Geophysical Research: Atmospheres, 108, 2003.

Deshler, T., Luo, B., Kovilakam, M., Peter, T., and Kalnajs, L. E.: Retrieval of aerosol size distributions from in situ particle counter measurements: instrument counting efficiency and comparisons with satellite measurements, Journal of Geophysical Research: Atmospheres, 2019.

Hu, Y., Rodier, S., Xu, K., Sun, W., Huang, J., Lin, B., Zhai, P., and Josset, D.: Occurrence, liquid water content, and fraction of supercooled water clouds from combined CALIOP/IIR/MODIS measurements, Journal of Geophysical Research: Atmospheres, 115, 2010.

Lamarque, J.-F., Dentener, F., McConnell, J., Ro, C.-U., Shaw, M., Vet, R., Bergmann, D., Cameron-Smith, P., Doherty, R., and Faluvegi, G.: Multi-model mean nitrogen and sulfur deposition from the Atmospheric Chemistry and Climate Model Intercomparison Project (ACCMIP): evaluation historical and projected changes, 2013.

Tan, J., Fu, J. S., Dentener, F., Sun, J., Emmons, L., Tilmes, S., Sudo, K., Flemming, J., Jonson, J. E., and Gravel, S.: Multi-model study of HTAP II on sulfur and nitrogen deposition, Atmospheric Chemistry and Physics, 18, 6847–6866, 2018.

Thomason, L. W., Ernest, N., Milln, L., Rieger, L., Bourassa, A., Vernier, J.-P., Manney, G., Luo,

B., Arfeuille, F., and Peter, T.: A global space-based stratospheric aerosol climatology: 1979-2016, Earth System Science Data, 10, 469–492, 2018.

Vet, R., Artz, R. S., Carou, S., Shaw, M., Ro, C.-U., Aas, W., Baker, A., Bowersox, V. C., Dentener, F., and Galy-Lacaux, C.: A global assessment of precipitation chemistry and deposition of sulfur, nitrogen, sea salt, base cations, organic acids, acidity and pH, and phosphorus, Atmospheric Environment, 93, 3–100, 2014.